TECHNIQUES FOR UNDERSTANDING ENGINE INLET VORTICES USING CFD : MIXING WALL SLIP BOUNDARY CONDITIONS

Luis Gustavo Trapp, lgtrapp@gmail.com
Roberto da Motta Girardi, girardi@ita.br
Instituto Tecnológico de Aeronáutica – ITA – São José dos Campos, Brazil

Abstract. *The effects of the inlet vortex on engines operating near the ground have been studied for more than 50 years, but the phenomenon is not yet completely understood. Computational Fluid Dynamics (CFD) is used, on a DLR-F6 modified nacelle, to allow a more detailed look into the inlet vortex phenomenon. The evolution of CFD tools and computer hardware have allowed the study of nacelles on crosswind conditions near the ground with greater accuracy. The objective of this work is to present a new technique that allows the evaluation of phenomena that are highly influenced by vorticity generated on the walls. This technique is based on using the CFD ability to mix wall boundary conditions with and without slip, allowing it to show that together with the ground vortex, coexists a feeding vortex that consists of vorticity created on the nacelle external surfaces and merges with the ground vortex inside the engine inlet .*

Keywords*: vortex, nacelle, engine, inlet, CFD, vorticity*

1. INTRODUCTION

Jet engines are adversely affected when operating near the ground in crosswind conditions, especially at high power. The high power static engine is affected by crosswind through three different ways: fuselage vortex shedding, inlet separation and ground vortex. All these phenomena produce a non-uniform airflow that is ingested by the inlet, which affects the engine operation, being able even to affect its physical integrity. This non-uniform flow ingested by the engine is generally referred to as “inlet distortion” or “distortion”, which is usually assessed through standard procedures, e.g. SAE, 1999.

The ground vortex forms between the engine inlet and the ground, at very low aircraft speeds and is created by the interaction between the inlet flow and the crosswind, being able to suck considerable large objects into the engine. It can also affect engine operability, when it is ingested by the engine core.

If the engine is operating near the ground, at high power, the stream tube ingested by the engine will induce flow on the ground, which can create a ground vortex: a strong vortex that builds up between the ground and the engine. The ground vortex is able to lift particles from the ground which are much larger than the ones carried by the average inlet flow, because of the vortex higher flow speed and lower pressure compared to the neighboring flow.

Over the last 50 years many authors have studied inlet vortices, either through experimental (Rodert and Garrett, 1955; Klein, 1959; Glenny and Pyestock , 1970; De Siervi , 1981; Liu, Reitzer and Tan, 1985; Shin et al. 1986; Brix, Neuwerth and Jacob, 2000, Murphy, 2008); or numerical means (Nakayama and Jones, 1999; Tourrette, 2002; Yadlin and Shmilovich, 2006; Trapp et al., 2007; Rehby, 2007; Trapp and Girardi, 2010).

The first author to propose the minimum requirements for a ground vortex to exist was Klein, 1959, conditioning it to the existence of:

1. A stagnation point on the ground (or other fixed structure), where an omni-directional air flow parallel to the surface converges, in a manner similar to a sink;
2. An updraft from the stagnation point to the inlet;
3. The presence of the ambient vorticity.

The evolution of Computational Fluid Dynamics (CFD) tools and computer hardware have allowed the study of nacelles on crosswind conditions near the ground with increased accuracy, greater stability and faster turn around. It allows a detailed look into the physical phenomenon, with a greater control than the one allowed in wind tunnels. The objective of this work is to present a new technique that allows the evaluation of phenomena that are highly influenced by vorticity generated on the walls. This technique is based on using the CFD ability to mix wall boundary conditions with and without slip.

Fig. 1 Ground vortex on an YC-14 aircraft (Campbell and Chambers, 1999)

2. CFD ANALYSIS

The inlet vortices simulations were performed using the DLR F6 nacelle (DLR, 2006), a wind tunnel model, long duct scaled nacelle model, from the wing-body-pylon-nacelle configuration used in the "AIAA Drag Prediction Workshops". Because this nacelle geometry is open to the general public it can be used in the future to compare results from different authors. The original nacelle is a hollow through-flow nacelle (TFN) which does not contain an engine. In order to use this nacelle model in an actual crosswind CFD simulation, the internal geometry was modified to better represent a real engine, incorporating outlet and inlet boundaries, but no effort was made to add a spinner at the fan plane. Typical dimensions for the DLR-F6 wind tunnel model nacelle are given on Table 1, together with design parameters. There are two major inlet design parameters that impact the smoothness of the flow that will reach the engine: the inlet diffuser ratio and the inlet contraction ratio. The inlet diffusion ratio is the ratio between the fan and the inlet throat areas, and it influences the air flow speed on the fan blades. The inlet contraction ratio is defined as the ratio between the inlet highlight and the inlet throat areas and regulates the flexibility of the inlet to ingest flows that are not aligned with the inlet plane, for example high angle of attack and crosswind conditions. The values of the DLR-F6 nacelle inlet diffusion and contraction ratios are also shown on Table 1. Additionally the inlet lip shape also influences the inlet flow separation margins, usually and an elliptical cross-section is used to avoid separation under crosswinds.

Given that the DLR-F6 was not specifically designed for crosswind conditions (it has a circular inlet lip cross-section and a low contraction ratio), it was modified to be more crosswind resistant, by increasing the highlight diameter and modifying the inlet lip cross-section into a 2.5 to 1 ellipse, while keeping the other parameters the same (see DLR MOD parameters on Table 1).

Table 1 DLR-F6 nacelle dimensions and design parameters

Design Parameter	Symbol	DLR-F6	DLR MOD
Length (mm)	L	180.0	
Inlet Throat Diameter (mm)	D_i	49.4	
Fan Diameter (mm)	D_f	54.8	
Max Diameter (mm)	D_m	76.2	
Exhaust Diameter (mm)	D_{ex}	50.0	
Diffusion ratio	DR	1.10	
Highlight Diameter (mm)	D_h	55.1	57.2
Contraction ratio	CR	1.24	1.34
Lip aspect ratio	LAR	1	2.5

In order to assess the nacelle behavior during crosswind operation, it was chosen, as typical condition, sea level, aircraft static, ISA day and a 90° crosswind, with wind intensities between 5 and 30 knots. The nacelle was positioned at a distance from the engine centerline to the ground equal to the highlight diameter. The computational domain was hemispherical, with a diameter 50 times the nacelle maximum external diameter.

The CFD analysis were performed using CFD++ (Metacomp, 2007), a commercial CFD software based on a finite-volume formulation, which can deal with arbitrary mesh types. The Reynolds−Averaged-Navier−Stokes three-dimensional equations are solved for the compressible flow using implicit, second order interpolation, centroidal based polynomials and pre−conditioned relaxation. The turbulence model used was realizable k-ε.

A hybrid tetra-prism mesh was used, and the CFD++ nodal interpolation polynomial. The hybrid grids for the isolated nacelle near the ground contained more than six million elements. The prism layer contained 25 elements with a growth ratio of 1.25. The parameter y+, which is important in evaluating the ability of the grid to capture near-wall effects, was of the order of 1 in all viscous cases. This mesh can be seen on Figures 2 and 3.

At the fan face boundary a mass flow rate boundary condition was used. The mass flow rate imposed was typical of an engine at the same condition, in this case 0.34 kg/s. The domain initial conditions were identical to the far field boundary conditions, at which a characteristic based velocity inflow/outflow was prescribed, imposing wind speed, temperature, turbulent intensity and turbulent length.

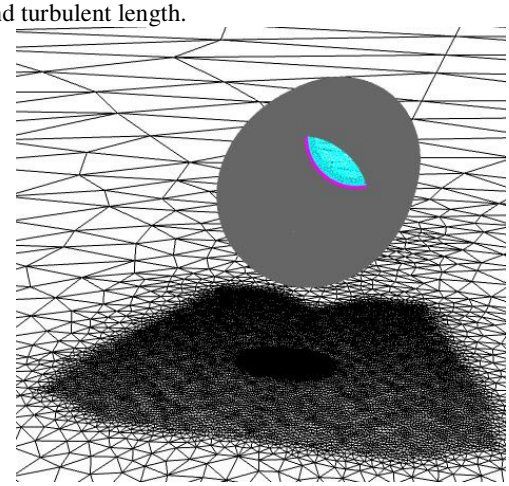

Figure 2 – View of the nacelle and the ground mesh

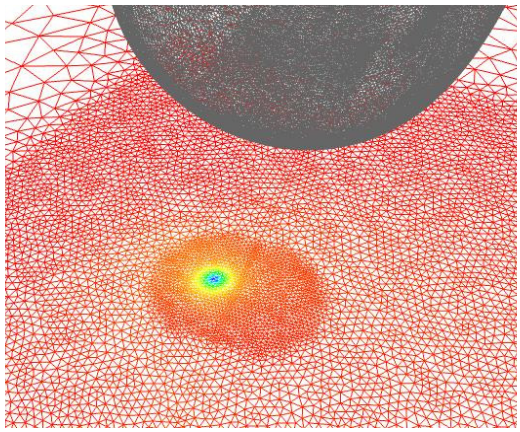

Figure 3 – Zoomed view of the mesh on the ground near the nacelle

One of the earlier problems that were faced, after running a CFD analysis with a ground vortex present, was to determine the best way to visualize it. An extensive analysis of current vortex visualization methods was performed (Trapp et al. 2007) in order to determine the best method or tool. The best way found was the 'vortex core' tool used in the Ensight visualization software (Ensight, 2005), which showed the best vortex characterization, without much noise or interference with other surfaces. However it still fails to predict the curved vortex core segments, therefore not capturing the ground vortex well on the region where it is turning more steeply into the engine. A turn around to this problem is to release particle traces from the vortex core, which will approximately show the vortex path. Other problem with this method is that it requires operations to be performed within the mesh grid, which is difficult to implement on a commercial post-processing code, if the code does not include this feature originally.

Trapp and Girardi, 2010, proposed a parameter, called the streamtube diameter ratio (SDR) to evaluate the relationship between the interference between the inlet streamtube with the ground and its effect on the inlet vortex strength. The SDR, as shown in Figure 4, is the ratio between the ideal streamtube diameter (D_0) and the diameter of an imaginary cylinder of radius equal to the distance from the engine axis to the ground (H). The ideal streamtube is the axis-symmetrical streamtube of an isolated nacelle, undisturbed by the ground. This definition implies that when the SDR is greater than one the inlet streamtube encompasses the ground and an inlet vortex may exist.

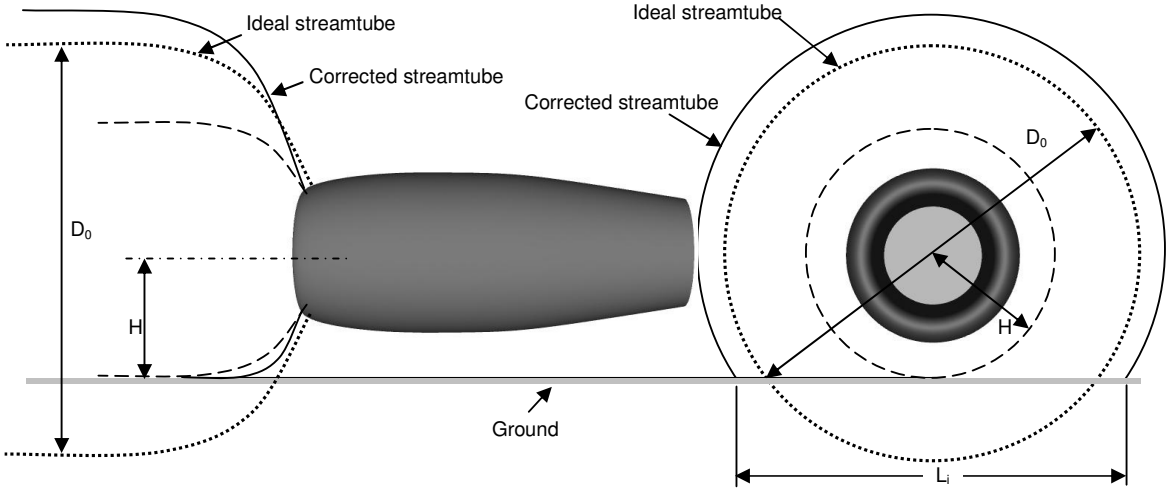

Figure 4 – Parameters involved on the definition of the Streamtube Diameter Ratio (SDR).

Additional cases were run to evaluate how the vortex intensity varied not only as a function of the SDR, but also as a function of the inlet mass flow rate, the crosswind intensity and the distance from the inlet to the ground. The circulation as calculated using the Stokes theorem:

$$\Gamma = \int_A \vec{\omega} \cdot \vec{n}\, dA \tag{1}$$

Where Γ is the circulation, $\vec{\omega}$ is the vorticity vector, A is the integration area and $\vec{n}$ is the vector normal do the integration area. The circulation can be made non-dimensional (Γ^*) by dividing it by the inlet throat diameter (D_{th}) and the freestream speed (U_∞):

$$\Gamma^* = \frac{\Gamma}{D_{th} U_\infty} \tag{2}$$

Figure 5 shows results of non-dimensional circulation for the following cases: (a) 20 knots crosswind, inlet height ratio of 1.03 and different engine mass flow rates; (b) 20 knots crosswind, height ratio of 1.13 and different engine mass flow rates; (c) inlet mass rate of 0.40 kg/s, height ratio of 1.13 and different crosswind intensities; (d) inlet mass rate of 0.34 kg/s, height ratio of 1.13 and different crosswind intensities.

The SDR showed that three inlet vortex regimes exist: a weak vortex regime between SDR 1.1 and 1.4 with minimum ground pressures close to the ambient pressure; a transient regime between 1.4 and 1.6, where the minimum pressure dropped suddenly; and a strong vortex regime at SDR greater than 1.6.

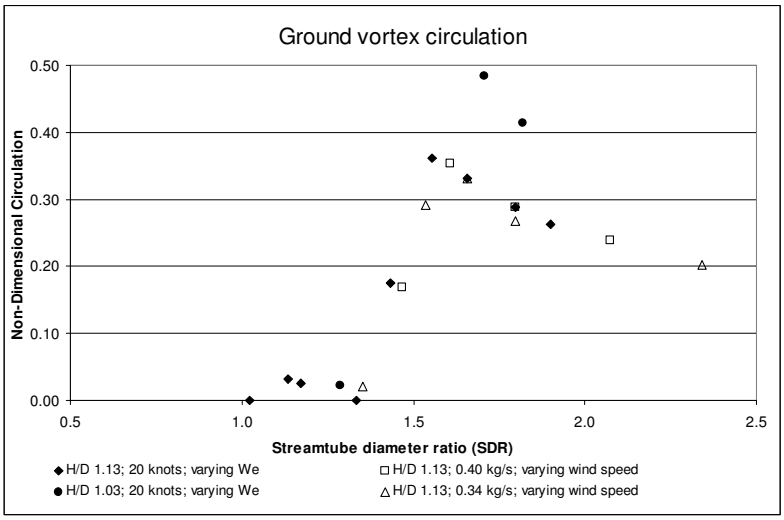

Figure 5 – Ground vortex non-dimensional circulation as function of the SDR, with different scenarios.

The ground vortex contains vorticity created on both ground and nacelle walls. However it is not clear the how these walls influence the vortex strength. Additionally, if the nacelle walls have any influence on the vortex intensity, it is useful to understand whether this influence is caused by the whole nacelle surface, or some parts of the nacelle have a greater influence on the ground vortex strength.

The methodology employed to understand the ground vortex phenomenon involved testing the different vorticity sources by changing the different domain walls between non-slipping and slipping boundary conditions. The slipping boundary condition, typically used to model solid surfaces in an inviscid-flow simulation, imposes a symmetry condition on the flow, in which all scalar and vector quantities are considered to be mirror-imaged in the planes defined by the surface-boundary faces. The flow velocity experiences a free slip at the boundary, becoming tangential to the surface on the boundary itself. When using this boundary condition, vorticity is not produced on the walls, therefore it is possible, by alternating selected surfaces, between slipping and non-slipping boundary conditions, to assess these surfaces influence on the ground vortex.

Initially four different cases were evaluated, all with 10 knots crosswind, 0.34 kg/s of inlet mass flow and a non-dimensional distance to the ground of 1.13: (a) standard case, where all walls are non-slipping; (b) the slipping nacelle walls case; (c) the slipping ground case; (d) the case with all walls slipping.

Figure 6 shows results for these cases: the standard case (a) resulted in a concentrated ground vortex; the slipping nacelle wall case (b) resulted in a vortex of similar diameter on the ground, but with a less vortex core suction; the slipping ground case (c) contains a vortex with similar core pressure, compared to the slipping nacelle vortex, but spreading through a larger area; (d) the case with all walls slipping, showed no vortex at all.

Therefore for the ground vortex to exist, a source of vorticity must be present in the flow. If the non-slipping condition is set on either the ground or the nacelle wall, this vorticity source exists and a ground vortex will form; however if only slipping walls boundary conditions are used, there will be no vorticity production and no ground vortex will form. The case with the ground slipping, but with the nacelle walls non-slipping, has a ground vortex, meaning that vorticity created on the nacelle walls influence the ground vortex.

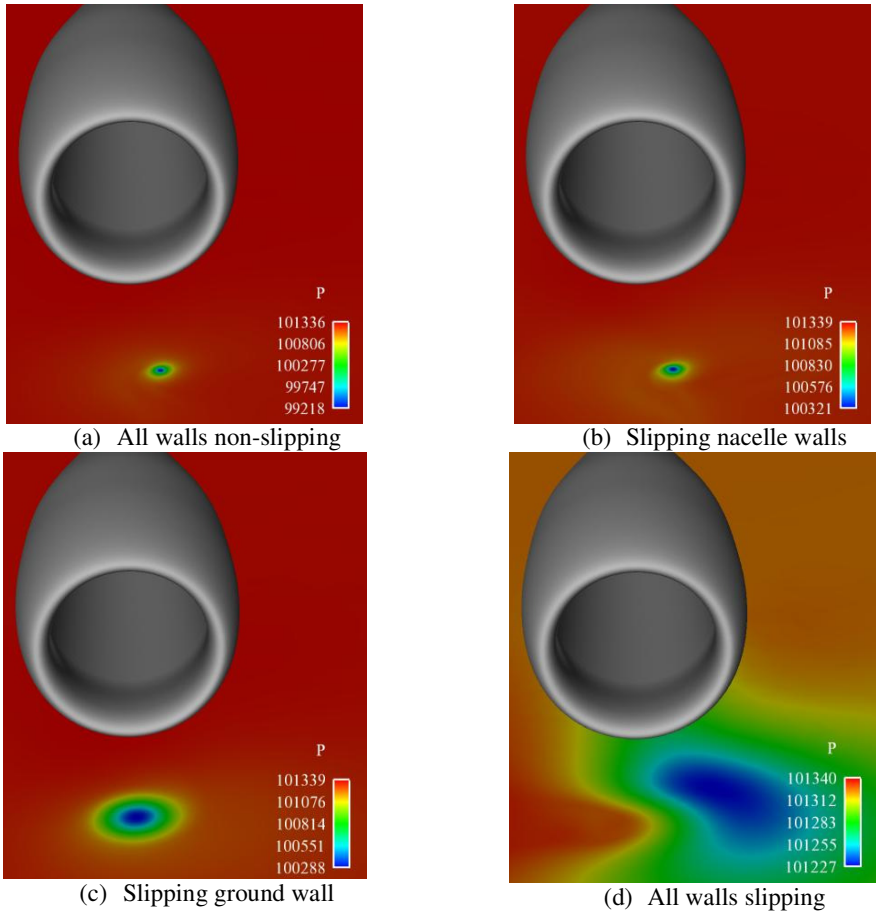

(a) All walls non-slipping (b) Slipping nacelle walls

(c) Slipping ground wall (d) All walls slipping

Figure 6 – Ground pressures for different wall boundary conditions.

Figure 7 shows vortex streamlines colored by vorticity intensity for the (a) all walls slipping, (b) ground slipping and (c) nacelle walls slipping cases. The stream lines are released from a vorticity isocurve created at a plane 40% of the distance between the ground and the hilite, with 90% of the peak vorticity at that plane. Figure 7(a) shows a different vortex shape than the one with a non-slipping ground (Figure 7 (b)), because the ground does not generate vorticity and the vortex boundary is able to spread without being dissipated by the ground shear, the vortex core being large and shallow on the ground, rather than concentrated as with the non-slipping ground. When all the walls are slipping (Figure 7 (c)), there is still a convergence of streamlines into the inlet, however the minimum vorticity levels are not enough to induce the streamlines to rotate and form a ground vortex.

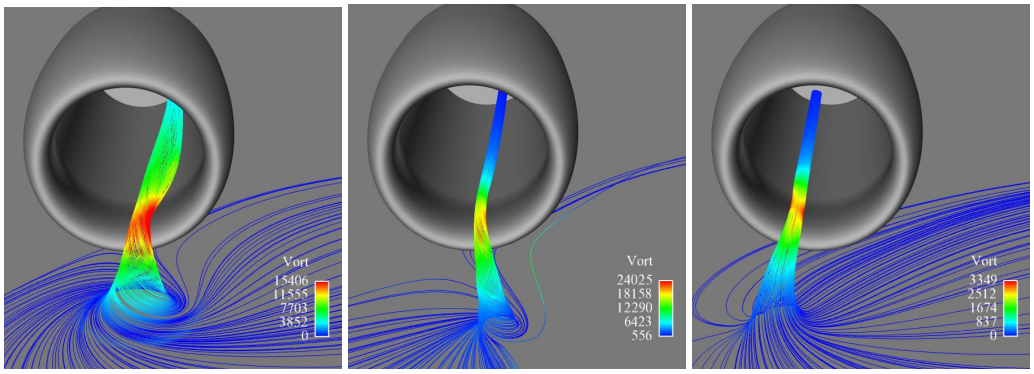

(a) (b) (c)

Figure 7 – Vortex streamlines colored by vorticity intensity for the (a) ground slipping; (b) nacelle walls slipping; (c) all walls slipping.

A comparison of the vorticity at the same height (20%) shows that the peak vorticity occurs on the no slip case, while the ground slip case has the minimum vorticity peak, but it spreads over a larger area (Figure 8). The slipping ground case has the largest core, with a vorticity peak much lower than the other cases, however given that its area is much greater than the other cases, varying with the square of the radius, it has the highest circulation. Both slipping nacelle and no slip cases have vortex cores of about the same diameter, showing how the ground shear is a major factor that dominates the vortex core radial spread.

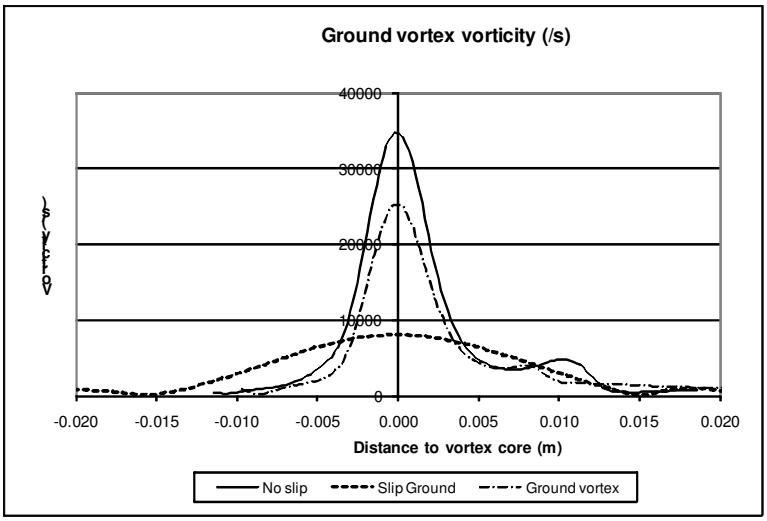

Figure 8 – Vorticity distribution relative to the vortex center for the different wall boundary condition combinations.

Figure 9 shows the ground vortex circulation at different ground heights (h), adimensionalized by the engine diameter D, for the different case – the 0% is the ground level, and the 35% approximately the bottom of the inlet lip. The first conclusion from this plot is that the inlet vortex looses intensity as it approaches the inlet, the closer it is to the inlet, the higher the losses – this is due to vortex stretching that decreases the vortex radius, while increasing the core velocity gradient, that then increases vortex dissipation. The highest circulation is present on the 'ground slip' case, implying that the ground, rather than strengthening the inlet vortex, by generating vorticity that will be incorporated in the inlet vortex, causes the vortex to lose strength, due to shearing between the vortex and the ground.

The case where the nacelle walls are slipping and all vorticity comes from the ground has an inlet vortex with the lowest circulation, even though a lot of vorticity is being produced on the ground, the ground shear layer is at the same time dissipating it. The case where all walls are no-slip, have the second greatest vortex intensity, showing that a major responsible for the inlet vortex strength are the nacelle walls, whereas the ground have a detrimental effect. Additionally, as already observed on the previous figures, the case where all the walls are slipping, produce no inlet vortex, and this is reflected on the plot below, where a very small circulation is seem on the 'all slip' case.

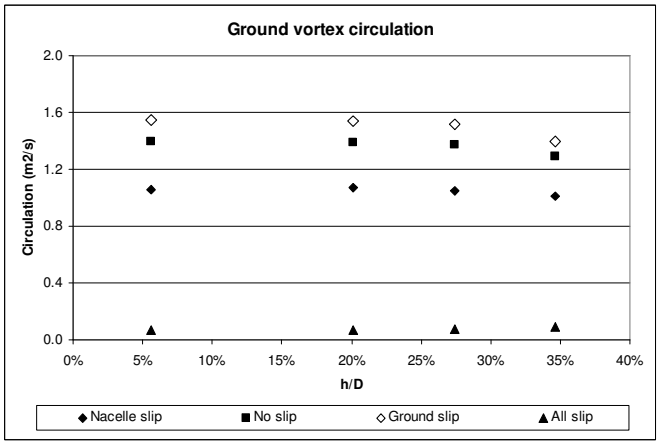

Figure 9 - Ground vortex circulation as a function of measurement plane height

An additional use of the capability of mixing slipping and non-slipping wall boundary conditions using CFD, is to apply them on the same surface. In this case a mesh was created, where the front of the nacelle, the region from the hilite to the maximum nacelle diameter, was split in 4 equal longitudinal length sectors. Then the rest of the nacelle was split into slices with the same length as the front (Figure 10), the last sector (12^{th}) was merged with the rest of the 13^{th} sector, which was smaller than the reference length.

CFD runs were performed with the sectors with different combinations of slipping and non-slipping boundary conditions. This methodology allowed pin pointing the major features that influence the inlet vortex and study the role that the nacelle surface plays on the strengthening of the inlet vortex.

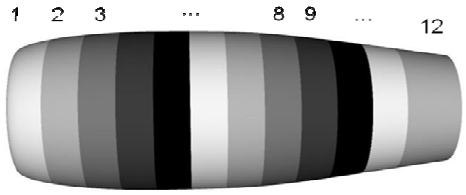

Figure 10 – Nacelle with splitted external walls.

A series of cases were ran with a 10 knots crosswind, where the nacelle slices were successively turned from non-slipping boundary conditions into slipping boundary conditions, from the nacelle hilite to the nacelle trailing edge (i.e. first a case with the first slice slipping and the other slices non-slipping was run, then the first and second slipping, the rest non-slipping, etc.). All other walls were kept slipping, which include the ground and the internal side of the nacelle, from the inlet hilite to the fan boundary condition (mass flow outlet), meaning that the external surface of the nacelle is the only surface generating vorticity in the CFD domain.

Figure 11 shows results for the case where the first three sectors have slipping walls, while the other sectors are non-slipping. It contains isolines of constant vorticity on planes passing to the center of each sector. The external vorticity downstream of the nacelle, like in a cylinder, accumulates in a wake and it is progressively sucked by the inlet. While it is being sucked, the wake gets further concentrated and the vorticity is intensified by vortex stretching. The isolines depict the location of the wake behind the nacelle and how this wake is further concentrated on the forward portion of the inlet. The location of the center of the top wake, which forms the trailing vortex, moves to the back of the nacelle, as the flow approach the inlet lip.

A more detailed look on the concentrated vorticity region in the front of the nacelle lip shows that two vortices coexist, a bigger ground vortex and on its side a smaller vortex, which we have called the feeding vortex.

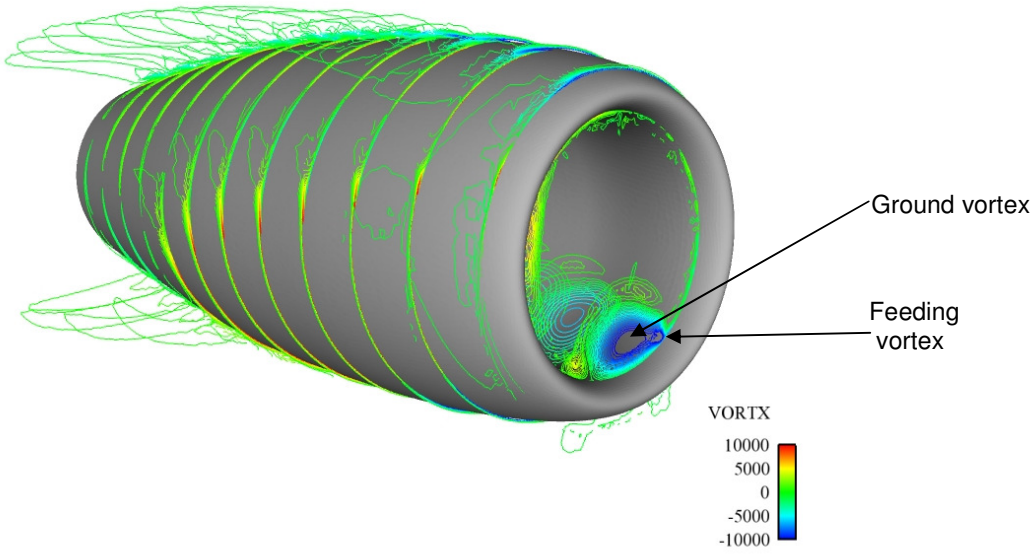

Figure 11 – Splitted nacelle with the three first sectors with wall slipping boundary conditions. The isolines of constant vorticity on planes are on the center of each sector.

Figure 12 shows, for the same case, isosurfaces of constant longitudinal vorticity, colored by longitudinal vorticity intensity, the nacelle surfaces is colored using two shades of gray, the lighter gray shows extend of the slipping sector, whereas the darker one (only visible close to the nacelle stagnation line) shows the non-slipping surfaces. There is vorticity being produced in the non-slipping sectors of the nacelle, the flow that is going through the top of the nacelle is producing negative vorticity, the bottom positive longitudinal vorticity. This positive longitudinal, as is being sucked by the engine and reaches the slipping wall region, ceases to produce vorticity and the wind component keep flowing to the nacelle circumferentially, forcing the longitudinal vorticity to accumulate in a narrow channel that is sucked by the inlet – this vorticity channel is the feeding vortex.

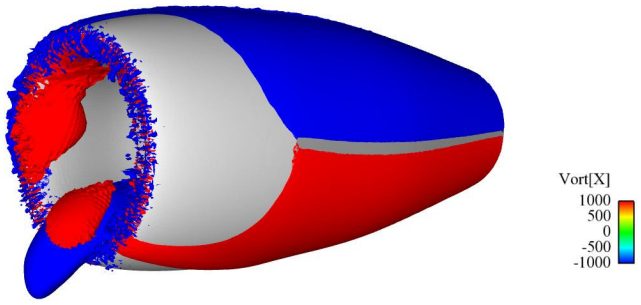

Figure 12 – Isosurfaces of constant longitudinal vorticity, colored by longitudinal vorticity intensity. Case with the first three sectors slipping (lighter gray shows extend of the slipping sector).

As more sectors are turned into slipping walls the ground vorticity incrementally loses intensity until finally disappearing, much like Figure 7(c) previously shown. This implies that the vorticity produced by the external nacelle surface has a major role on the ground vortex existence.

3. CONCLUSIONS

A universal relationship between the vortex intensity and the inlet streamtube was shown and it seems to take into account the major parameters in the inlet vortex phenomenon, namely the inlet distance to the ground, the engine inlet flow and the crosswind speed.

It was shown that it is possible to use, simultaneously, boundary conditions of slipping and non-slipping types to identify how the local production of vorticity influences the overall flow. The use of these boundary conditions side-by-side has not influenced the solver behavior and did not cause any convergence or instability problems. More over they have allowed to pin point the most important regions that contribute for the existence of an inlet vortex.

For the ground vortex to exist, a source of vorticity must be present in the flow. If the non-slipping condition is set on either the ground or the nacelle wall, this vorticity source exists and a ground vortex will form; however if only slipping walls boundary conditions are used, no ground vortex will form. The vorticity created on the nacelle external wall contribute more for the ground vortex intensity than the ground.

The subdivision of the nacelle external walls into many sectors has allowed the identification a region of concentrated vorticity, that is sucked by the inlet and merges into the ground vortex. This concentrated vorticity region has been called *feeding vortex*, as it seems to a source of vorticity for the ground vortex. Once the feeding vortex does not exist, as when the nacelle external surface has slipping boundary conditions, the ground vortex ceases to exist.

4. REFERENCES

Brix, S., Neuwerth, G., and Jacob, D., “The inlet-vortex system of jet engines operating near the ground”, AIAA Paper 2000-3998, Jun. 2000.

Campbell, J.F., and Chambers, J.R. “Patterns in the sky: natural visualization of aircraft flow field”s, NASA, Langley Research Center, USA, 1994.

De Siervi, F., “A flow visualization study of the inlet vortex phenomenon”, MSc Dissertation, Massachusetts Institute of Technology, USA, 1981.

DLR F6 Geommetry. 2nd AIAA Drag Prediction Workshop, Orlando, USA, 2006. URL: http://aaac.larc.nasa.gov/tsab/cfdlarc/aiaa-dpw/Workshop2/DLR-F6-geom.html [retrieved 02 January 2008].

Ensight, “User’s Manual for Version 8.0”, Computational Engineering International, Inc., Apex, USA, 2005.

Glenny, D.E., and Pyestock, N.G.T.E., “Ingestion of debris into intakes by vortex action”, Aeronautical Research Council, London, Current Papers No. 1114, 50 pp, 1970.

Klein, H. J., Douglas Aircraft Company, US Patent for “Vortex Inhibitor for Aircraft Jet Engines”, No. 2,915,262. B64D33/02, filed 01 Dec 1959.

Liu, W., Reitzer, E.M., and Tan, C.S., "Surface static pressures in an inlet vortex flow field", Journal of Engineering for Gas Turbines and Power, vol. 107, p. 387-93, 1985.

Metacomp Technologies, "CFD++ v.7.1.1 User Manual", Metacomp Technologies, USA, 2007.

Murphy, John. "Intake Ground Vortex Aerodynamics", PhD thesis, Cranfield University, Cranfield, United Kingdom, 2008.

Rehby, L. "Jet engine ground vortex studies", MSc Dissertation, Cranfield University, Cranfield, United Kingdom, 2007.

Rodert, L.A., and Garrett, F.B., "Ingestion of foreign objects into turbine engines by vortices", NACA TN-3330, Washington, USA, 1955.

SAE, "Inlet Total-Pressure-Distortion Considerations for Gas-Turbine Engines", Society of Automobile Engineers Aerospace Information Report 1419, Rev. A., 1999.

Shin, H.W., Greitzer, E.M., Cheng, W.K., Tan, C.S., and Shippee, C.L., "Circulation measurements and vortical structure in an inlet-vortex flow field", Journal of Fluid Mechanics, Vol. 162, pp. 463-87, 1986.

Tourrette, L., "Navier-Stokes simulations of air-intakes in crosswind using local preconditioning", AIAA Paper No. 2002-2739, June 2002.

Trapp, L.G., Argentieri, H.G., Souza, F.J. and Girardi, R.M., "Wind effects on isolated nacelles near the ground", Proceedings of th 11th Brazilian Congress of Thermal Sciences and Engineering, Curitiba, Brazil, 2006.

Trapp , L.G., Girardi , R.M., " An engine nacelle in crosswind: the inlet vortex", Journal of Aircraft, vol.47, no.2, pp 577-90, 2010.

Yadlin, Y., and Shmilovich, A., "Simulation of Vortex Flows for Airplanes in Ground Operations", AIAA Paper No. 2006-0056, Jan. 2006.

5. RESPONSIBILITY NOTICE

The authors are the only responsibles for the printed material included in this paper.